

JoVE: Science Education
Buoyancy and Drag on Immersed Bodies
--Manuscript Draft--

Manuscript Number:	10392
Full Title:	Buoyancy and Drag on Immersed Bodies
Article Type:	Manuscript
Section/Category:	Manuscript Submission
Corresponding Author:	Alexander Rattner UNITED STATES
Corresponding Author Secondary Information:	
Corresponding Author's Institution:	
Corresponding Author's Secondary Institution:	
First Author:	Alexander Rattner
First Author Secondary Information:	
Order of Authors:	Alexander Rattner
Order of Authors Secondary Information:	

PI Name: Alexander S Rattner, Sanjay Adhikari

Science Education Title: Buoyancy and Drag on Immersed Bodies

Overview

Objects, vehicles, and organisms immersed in fluid mediums experience forces from the surrounding fluid in the form of *buoyancy* – a vertical upward force due to fluid weight, *drag* – a resistive force opposite the direction of motion, and *lift* – a force perpendicular to the direction of motion. Prediction and characterization of these forces is critical to engineering vehicles and understanding the motion of swimming and flying organisms.

In this experiment, the balance of buoyancy, weight, and drag forces on submerged bodies will be investigated by tracking the rise velocity of air bubbles and oil droplets in a glycerin medium. The resulting drag coefficients at terminal rise velocities will be compared with theoretical values.

Principles

When a body rises in a fluid medium, it experiences the external forces of gravity, buoyancy, and fluid drag. The force from gravity is weight (W), and acts downward with magnitude $W = mg$ (m is the mass of the body, and g is the gravitational acceleration, 9.8 m s^{-2}).

The buoyancy force (F_b) acts upward, opposing gravity. Pressure increases with depth in a fluid medium due to the greater weight of fluid above deeper points in the medium. Thus, the pressure force acting upward on the bottom of an immersed body is greater than the pressure force acting downward on the top of the body, resulting in the upward buoyancy force. The buoyancy force magnitude is $F_b = \rho_f V g$, where ρ_f is the density of the surrounding fluid medium and V is the volume of the immersed body. This is equal to the weight of fluid displaced by the submerged body.

When a body moves through a fluid medium, it experiences frictional resistance from the fluid, called *drag*. The drag force (F_D) acts opposite to the direction of motion, and depends on the shape and size of the body, its velocity, and the fluid properties. In general, drag force can be modeled as:

$$F_D = \frac{1}{2} C_D (\text{Re}) \rho_f U^2 A \quad (1)$$

Here, U is the velocity of the immersed body and A is the face area of the body (projected area in the direction of motion). C_D is the drag coefficient, which depends on the shape of the body and its Reynolds number – a measure of the relative magnitude of inertial and viscous fluid forces on the body. Here, $\text{Re} = \rho_f U D / \mu_f$, where D is a relevant length scale for the body (diameter for spheres and cylinders) and μ_f is the fluid viscosity.

In this experiment, air bubbles and oil droplets will be injected into a high viscosity glycerin bath, and rise to the free surface. A free body diagram on a bubble/droplet (Fig. 1) rising at the

terminal velocity (not accelerating) gives the vertical force balance: $F_B - W - F_D = 0$. Substituting earlier results, and assuming a spherical bubble (volume $V = (1/6)\pi D^3$, face area $A = (1/4)\pi D^2$) yields the following result (Eqn. 2). Here, ρ_b is the density of the fluid inside the bubble/droplet.

$$C_D = \frac{4}{3} \frac{Dg(\rho_f - \rho_b)}{\rho_f U^2} \quad (2)$$

In this experiment, the drag coefficient (C_D) for spheres will be measured based on the rise velocity of different size bubbles and droplets. These data will be compared with the theoretical result of [1,2] for low Reynolds numbers ($Re \lesssim 10$).

$$C_{D,theory} = \frac{16}{Re} \quad (3)$$

Procedure

1. Fabrication of gas injection test section (see schematic and photograph, Fig. 2)
 - 1.1. Drill a hole in the bottom of a tall, flat walled plastic container. Install a through-wall bulkhead fitting through this hole. Install a reducing fitting to a ~3.2 mm tube compression connection in the bulkhead fitting outlet. This will be the bubble/droplet injection port.
 - 1.2. Insert a short length (~1 cm) of 3.2 mm diameter soft rubber cord in the compression connection, and tighten the fitting nut. Using a sewing pin, puncture a thin hole through the rubber cord. This will be the valve for injecting bubbles/droplets into the fluid container.
 - 1.3. Fill the container with glycerin to a level of ~25 cm. Pour the glycerin slowly as a film down the container sidewall to help reduce bubble entrainment in the container. Wait for ~2 hours to allow larger bubbles to rise out of the container.
 - 1.4. Mount a video camera on a tripod facing the container, with the upper portion of the liquid in view. Mount a bright light on the other side of the container, facing the camera (backlighting). Insert a diffuser sheet between the light and container to ensure even illumination.
2. Performing experiments
 - 2.1. Insert a ruler or flat object of known size into the glycerin container, above the injection port, facing the camera. Record a brief video of the object. This will serve a scale to map from bubble size in px and rise velocity in px s^{-1} to m and m s^{-1} , respectively.
 - 2.2. Using a syringe with a thin needle (*e.g.*, 20 gauge). Inject gas bubbles of varying sizes through the rubber valve into the liquid. Use the camera to record videos of the bubbles rising through the liquid.

- 2.3. Mix oil-based food coloring with soybean vegetable oil (or other low-viscosity vegetable oil). Using the syringe, inject colored oil droplets of varying sizes into the glycerin container. Record videos of the droplets rising.
3. Analysis
 - 3.1. Using software such as VLC media player, export image snapshots from the video of the ruler (Step 2.1). In an image editing software measure the pixel distance across a known length of the device. The length scaling factor can then be determined as $s = L_m/L_{px}$, where L_m is the physical length of the object in meters and L_{px} is the object length in pixels in the image.
 - 3.2. For each bubble or droplet rise velocity video, extract image snapshots from when the bubbles/droplets enter and exit the camera view window. Measure the bubble/droplet (horizontal) diameters in an image editing software (D_{px}). Measure the average rise velocities (U_{px}) as the difference in bubble/droplet nose positions divided by elapsed video times between initial and final image snapshots. Convert these pixel values to physical values as: $D = sD_{px}$ and $U = sU_{px}$.
 - 3.3. Evaluate bubble and droplet Reynolds numbers ($Re = \rho_f UD / \mu_f$) and drag coefficients (Eqn. 2). Plot these values and compare with theoretical results from Eqn. 3. Fluid properties at room temperature (22°C) are:
 - Glycerin: $\rho_f = 1300 \text{ kg m}^{-3}$, $\mu_f = 3.7 \text{ kg m}^{-1} \text{ s}^{-1}$
 - Air: $\rho_b = 1.19 \text{ kg m}^{-3}$
 - Soybean oil: $\rho_b = 920 \text{ kg m}^{-3}$

Representative Results

A series of rising air bubbles and oil droplets of varying diameters are presented in Fig. 3. The small bubbles and droplets rise at lower velocities due to relatively stronger drag forces. At these low velocity and length scales, strong surface tension forces result in nearly spherical bubbles and droplets. The largest bubbles approach $Re \sim 2$, resulting in somewhat flattened tails in the wake region. The largest oil droplets only approach $Re \sim 0.2$ due to their greater weights. The large droplets form slightly teardrop shapes, likely due to the high inertia (density) of the oil circulating inside the droplets. In contrast, the low density air in the gas bubbles has negligible inertia.

Measured drag coefficients (Eqn. 2) are compared with theoretical values for air bubbles and oil droplets (Eqn. 3) in Fig. 4. The most significant sources of uncertainty in this study stem from the glycerin viscosity value, which varies sharply with temperature, and the diameters of the smallest bubbles/droplets. Here, uncertainty propagation is performed assuming $\pm 0.2 \text{ kg m}^{-1} \text{ s}^{-1}$ for glycerin viscosity (corresponds to $\sim \pm 1^\circ\text{C}$) and $\pm 1.5 \text{ mm}$ for bubble diameter ($\sim 3 \text{ px}$). Overall, qualitatively close agreement is observed with theory in Fig. 4, with most measured C_D values matching theoretical results within experimental uncertainty.

Summary

This experiment demonstrated the measurement of drag coefficient for rising bubbles and droplets in a fluid medium. Drag coefficients were determined by accounting for weight, buoyancy, and drag forces. Results were compared with a theoretical model for bubble/droplet C_D at low Reynolds numbers.

When analyzing the flows affecting small or deformable objects, such as bubbles and droplets, it is often necessary to indirectly measure lift and drag forces based on object velocity. When analyzing larger objects, such as airplane wings or car bodies, scale models can be mounted on fixed force gages in wind tunnels, and subjected to external flows. In such cases, drag (and lift) forces can be measured directly (Eqn. 1). Engineers apply such information to optimize the shapes of vehicles for reduced drag and ensure that engines provide sufficient power to overcome fluid resistance.

Applications

This experiment focused on the motion of bubbles and droplets in a liquid medium. These results could be directly applicable to the design of industrial heat and mass exchangers, such as steam generators in power plants. In steam generators, vapor bubbles must be removed from the heated area by buoyancy or fluid flow to allow fresh liquid to reach the heating elements. In chemical reactors, gas bubbles are often injected to improve mixing. Characterization of bubble motion through liquid is thus needed to inform system design.

Vehicles such as cars, planes, and boats experience significant forces from drag. For example, at highway speeds, a typical sedan may require ~40 horsepower just to overcome aerodynamic resistance. Careful design of vehicle shape and intake/exhaust pathways can control airflow around a vehicle and reduce drag. In boats, submarines, and hot air balloons/blimps the buoyancy force balances the vehicle weight and must be considered carefully. By applying the principles introduced here, we can predict weight, buoyancy, and drag forces in engineering systems.

Legend

Figure 1: Force balance on rising gas bubble or oil droplet

Figure 2: (a) Schematic and (b) photograph of experimental facility.

Figure 3: Image series of rising gas bubbles and oil droplets of varying diameters

Figure 4: Measured drag coefficients and Reynolds number for rising bubbles and droplets compared with theoretical model (Eqn. 3).

Materials List

Name	Company	Catalog Number	Comments
Equipment			
Acrylic container	Oxo	1071393	
Bulkhead fitting	McMaster	36895K161	For bubble/droplet injection port
Compression fitting adapter	Swagelok	B-200-1-8	For bubble/droplet injection port
Soft rubber cord (3.2 mm diameter)	McMaster	9407K12	For bubble injection valve
Syringe and 20 gage needle			
Lighting panel	StudioPRO	S-600D	Backlighting systems
Chemicals			
Glycerin (1-2 gal)	Essential Depot	892647002291	
Vegetable oil (Soybean oil)			
Oil-based food coloring	Chefmaster	750025 4211	Chefmaster red 4211 used here

References

- [1] J.S. Hadamard, Motion of liquid drops (viscous), Comp. Rend. Acad. Sci. Paris. 154 (1911) 1735–1755.
- [2] W. Rybczynski, On the translatory motion of a fluid sphere in a viscous medium, Bull. Acad. Sci., Cracow, Ser. A. (1911) 40.

Figure 1

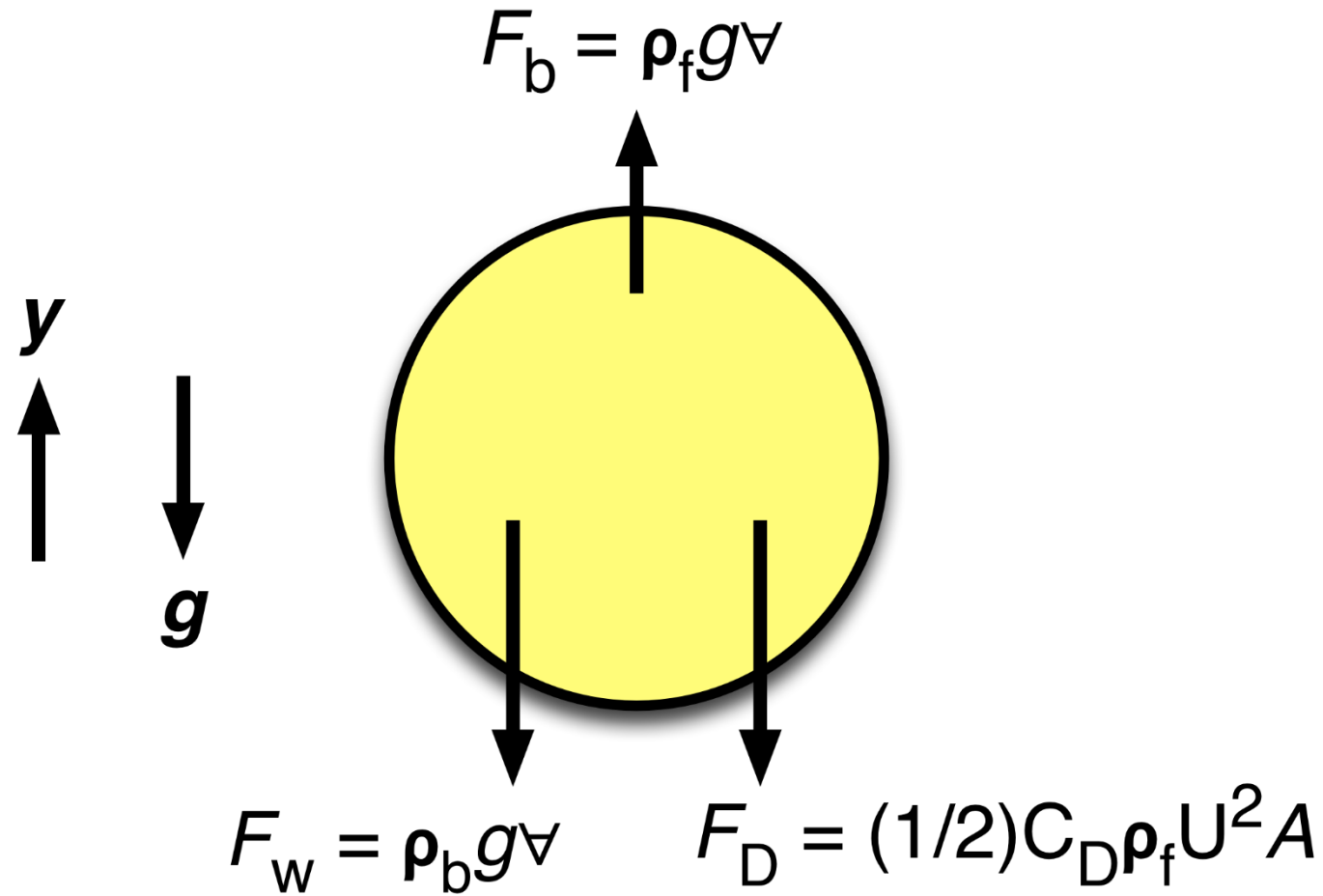


Figure 2

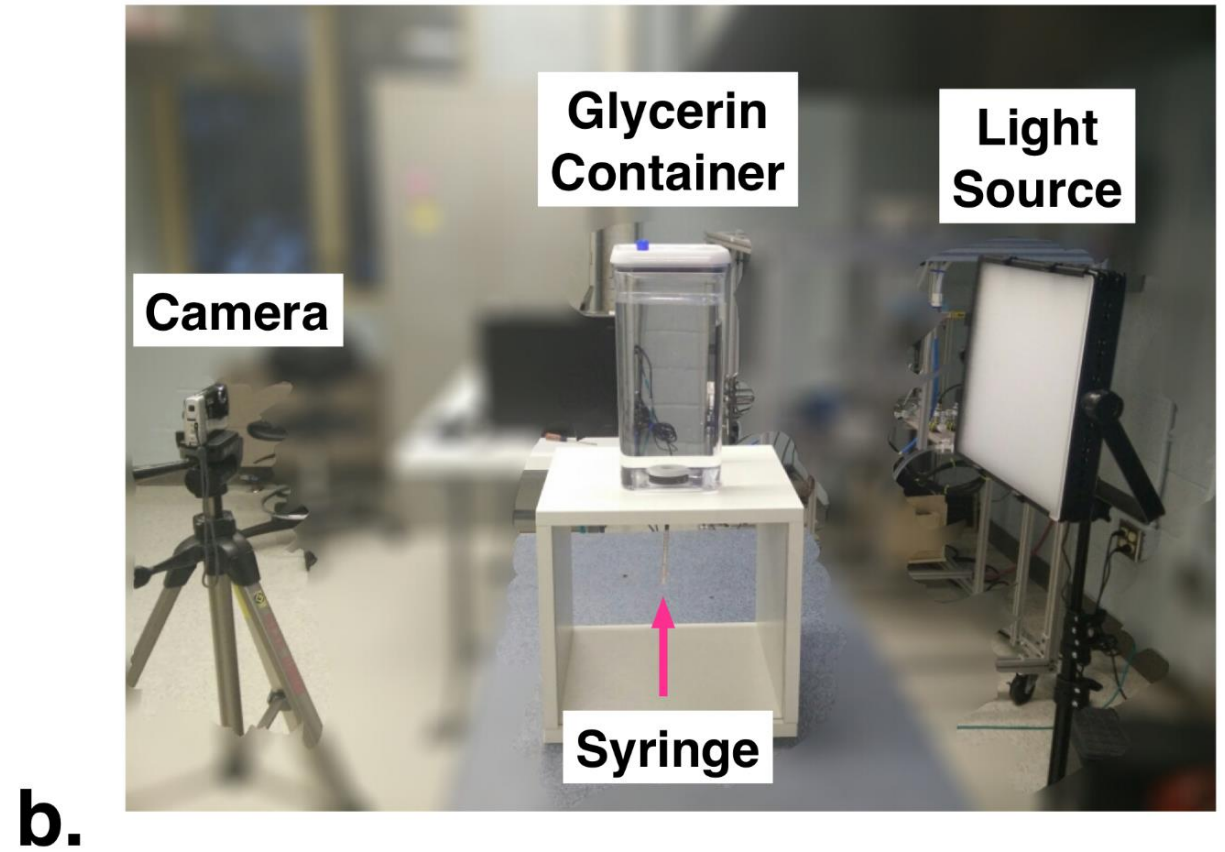
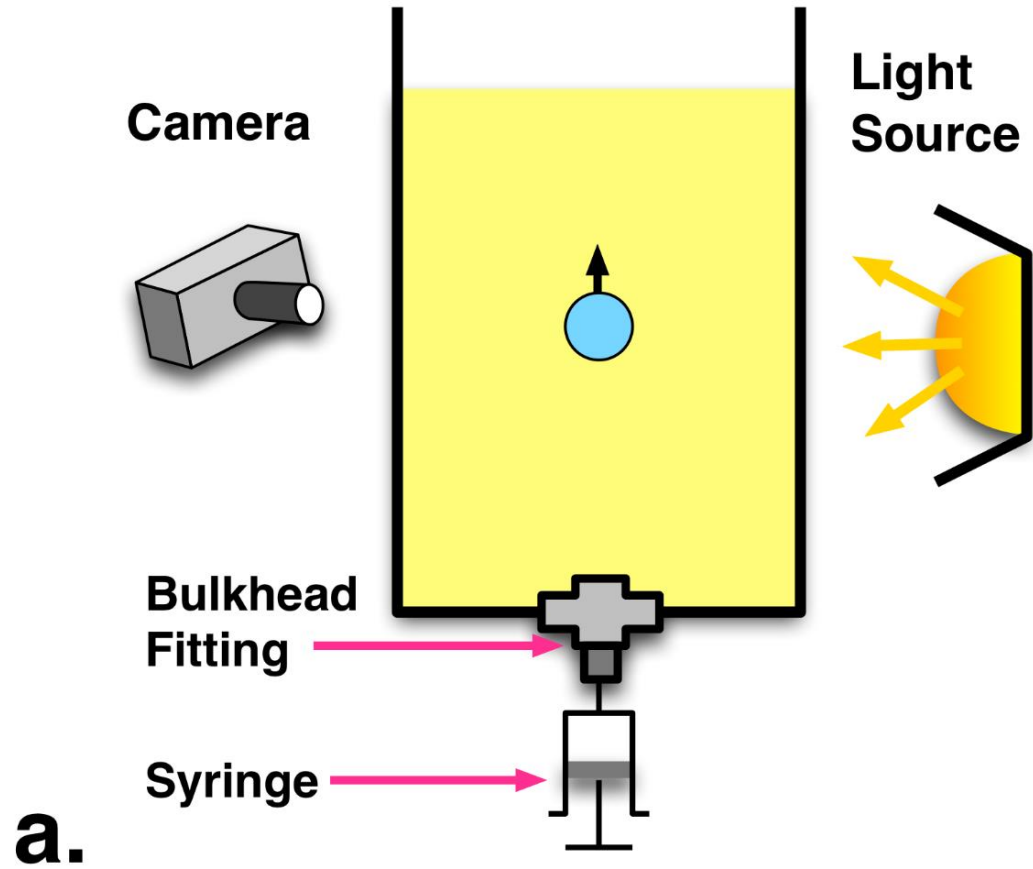
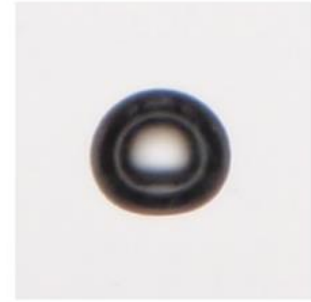
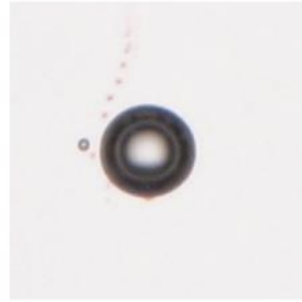
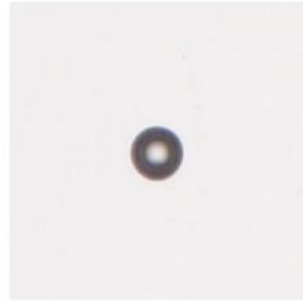
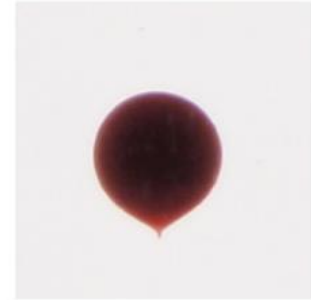
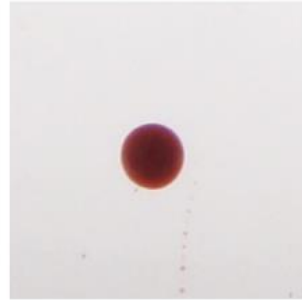
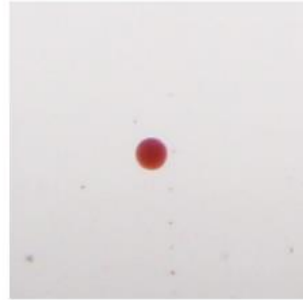


Figure 3

**Air
Bubbles**



**Oil
Droplets**



Increasing Diameter →

0.5 cm —

Figure 4

